




Use of infrared thermography to detect early alterations of peripheral perfusion: evaluation in a porcine model

MATHIEU MAGNIN,^{1,2}  STEPHANE JUNOT,^{1,3,*} MARTINA CARDINALI,^{1,3} JEAN YVES AYOUB,^{1,2} CHRISTIAN PAQUET,^{1,2} VANESSA LOUZIER,^{1,2} JEANNE MARIE BONNET GARIN,^{1,2} AND BERNARD ALLAOUCHICHE^{1,4}

¹ *Université de Lyon, APCSe Agressions Pulmonaires et Circulatoires dans le Sepsis, VetAgro Sup, F-69280 Marcy l'Etoile, France*

² *Université de Lyon, Vetagro Sup, Campus Vétérinaire de Lyon, Unité de Physiologie, Pharmacodynamie et Thérapeutique, F-69280 Marcy l'Etoile, France*

³ *Université de Lyon, VetAgro Sup, Campus Vétérinaire de Lyon, Anesthésiologie, F-69280 Marcy l'Etoile, France*

⁴ *Université de Lyon, Hospices Civils de Lyon, Centre Hospitalier Lyon Sud, Réanimation Médicale, Unité APCSE, Pierre-Bénite, France*

*stephane.junot@vetagro-sup.fr

Abstract: This study aimed to evaluate the variations of infrared thermography according to rapid hemodynamic changes, by measuring the peripheral skin temperature in a porcine model. Eight healthy piglets were anesthetized and exposed to different levels of arterial pressure. Thermography was performed on the left forelimb to measure carpus and elbow skin temperature and their associated gradient with the core temperature. Changes in skin temperature in response to variations of blood pressure were observed. A negative correlation between arterial pressure and temperature gradients between peripheral and core temperature and a negative correlation between cardiac index and these temperature gradients were observed. Thermography may serve as a tool to detect early changes in peripheral perfusion.

© 2020 Optical Society of America under the terms of the [OSA Open Access Publishing Agreement](#)

1. Introduction

Shock is defined as a life-threatening, generalized form of acute circulatory failure associated with inadequate oxygen utilization by the cells [1]. In this critical condition, circulation fails to deliver sufficient oxygen to meet the tissues demand. Circulatory failure may result from one, or an association, of the four following mechanisms: hypovolemia, cardiac dysfunction, generalized vasodilation or obstruction of blood circulation [1,2]. Circulatory shock is one of the leading causes of admission to intensive care unit with more than one third of the patients admitted with this condition [3]. In the time-course of circulatory failure, compensatory mechanisms occur to redistribute blood from non-vital organs to vital organs [1,4]. Clinically, this leads to signs of poor peripheral perfusion including decreased capillary refill time, cold extremities, skin mottling and decreased peripheral pulses [1,4–6]. An early recognition of these signs is important because the occurrence of a circulatory failure can rapidly lead to a multiple organ dysfunction syndrome and potential death [2]. For instance, the mortality rate associated with septic shock is about 30 to 80% [7].

Assessing early changes in peripheral perfusion can thus provide interesting information for the physician and allow a prompt initiation of supportive maneuvers. So far, the clinical signs afore-mentioned are performed at the patient's bedside and remain subjective. And objective means to assess peripheral perfusion with dedicated technologies are lacking.

Recently, the use of infrared thermography has been advocated to monitor peripheral perfusion: it has the advantage of being non-invasive, easy to use and cost-effective [4,8,9]. The measurement of peripheral and core temperature can allow the calculation of a gradient between both sites, with values between 3 and 7 °C considered as normal; any increase in this gradient may indicate a peripheral hypoperfusion [6].

Infrared thermography (IT) is a painless, non-ionizing, contact-free diagnostic imaging technique. It records the cutaneous thermal patterns generated by the emission of infrared radiation (IR). Every object whose temperature is greater than absolute zero carries energy in the form of IR. The emission of IR is proportional to the surface area of the object, its temperature, its environment and emissivity (ranging from 0 to 1). Human skin emissivity is about 0,98, which renders the human body an efficient infrared radiator [10,11]. This high emissivity of skin enables the use of thermography as a medical tool. It has been applied to assess organ perfusion during transplantation [12], thromboembolism [13,14] and vasculopathy secondary to diabetes [15] or Raynaud's disease [9].

The relationship between skin temperature and perfusion is complex. The skin temperature is the resultant balance between the heat transport within the peripheral tissues (dependent on blood circulation and local factors) and the heat loss to the environment (by radiation, conduction, convection and evaporation) [16,17]. The skin temperature is thus influenced by the core body temperature and environmental factors (ambient temperature, humidity). Consequently, any hemodynamic instability and its associated decrease in peripheral perfusion can cause changes in skin temperature, as illustrated by the coldness of the extremities observed during shock. Given these characteristics, the use of IT for the assessment peripheral perfusion in critical condition presents a potential interest.

This study aimed to evaluate the potential interest of IT as a tool to detect variations of peripheral perfusion associated with pharmacologically induced rapid hemodynamic changes, in a porcine model.

2. Materials and methods

2.1. Ethical statement

This study was conducted in accordance with the Guide for the Care and Use of Laboratory Animals and approved by the Ethics Committee of our institution (VetAgroSup, Marcy l'Etoile, France, authorization number: 1819).

2.2. Animals

Eight healthy piglets, weighing between 35 and 45 kg, 2 to 3 months old were included in the study. They were housed for a 7 days acclimatization period in an individual box. They were fed with standard food, with *ad libitum* access to water. Eight hours before the beginning of the experimental phase, solid food was withdrawn while free access to water was allowed.

2.3. Anesthetic protocol and surgical preparation

The study was performed in a research institute with a controlled environment. The experimental conditions were similar for every pig, with an ambient temperature of 25°C and a relative humidity of 50%. Animals were premedicated with intramuscular (IM) administration of a mixture of tiletamine-zolazepam (Zoletil100, 100 mg.mL⁻¹, Virbac, Carros, France) 3.0 mg.kg⁻¹ and morphine (Morphine Aguettant, 10 mg/mL⁻¹, Laboratoire Aguettant, Lyon, France) 0.2 mg.kg⁻¹. Twenty minutes later, propofol (Propovet 10 mg.mL⁻¹, Zoetis, Malakoff, France) 4.0 mg.kg⁻¹, was administered intravenously (IV) to effect *via* a catheter (Insyte-W 1.1 × 30 mm, Beckton Dickinson Vascular Access, Sandy, Utah, USA) placed in an auricular vein. After induction of anesthesia, animals were orotracheally intubated and placed under mechanical ventilation with a

controlled tidal volume set at $8.0 \text{ mL}\cdot\text{kg}^{-1}$ and an initial respiratory rate of $16 \text{ breaths}\cdot\text{min}^{-1}$. Anesthesia was maintained with sevoflurane (Sevoflo, Zoetis, Malakoff, France) in 30% oxygen, in association with an intravenous constant rate infusion (CRI) of morphine $0.1 \text{ mg}\cdot\text{kg}^{-1}\cdot\text{h}^{-1}$. The respiratory rate and tidal volume were adjusted to obtain an end tidal CO_2 of 4.6-6.0 kPa (35-45 mmHg). Intravenous fluids (Lactated Ringer) were administered throughout the experiment at a basal rate of $5 \text{ mL}\cdot\text{kg}^{-1}\cdot\text{h}^{-1}$.

After induction of anesthesia, the piglets were placed in dorsal recumbency on a heated table. It was ensured that the forelimbs of the animals were not in contact with the heating mattress. The external right jugular vein was dissected for placement of a central venous catheter (Multicath 3 7.5Fr, Vygon, Ecouen, France). A 4F thermodilution catheter (PiCCO catheter 5 Fr, Getinge, Orléans, France) was inserted into the lower abdominal aorta through the right femoral artery and connected to a PiCCO system.

2.4. Hemodynamics monitoring

The following hemodynamics parameters were measured: mean arterial pressure (MAP), systolic arterial pressure (SAP), diastolic arterial pressure (DAP), heart rate (HR), cardiac output (CO), systemic vascular resistance (SVR), global end-diastolic blood volume (GEDV), pulse pressure variation (PPV). Body surface area (BSA) was calculated as previously described [18]. Shock index (SI), cardiac index (CI), systemic vascular resistance index (SVRI) were calculated based on conventional equations ($\text{SI} = \text{HR}/\text{SAP}$; $\text{CI} = \text{CO}/\text{BSA}$; $\text{SVRI} = ((\text{MAP} - \text{CVP})/\text{CI}) \times 80$; CVP: central venous pressure). Global end-diastolic blood volume index (GEDVI) was calculated by indexing GEDV on the BSA. Hemodynamic parameters were continuously registered.

2.5. Study design

After equipment and stabilization of the animal, an initial fluid bolus (Ringer Lactate, $10 \text{ mL}\cdot\text{kg}^{-1}$ over 20 minutes) was administered to warrant the absence of preload dependence before the hemodynamic challenges. In case of fluid responsiveness, the fluid bolus was repeated, but only the last one was registered. A succession of hypotension and hypertension phases was then performed, as shown in Fig. 1. A hypotensive phase was induced by inhalation of an increased concentration of sevoflurane. Two hypertensive challenges were then performed by a CRI of norepinephrine. For each pig, 10 coupled thermographic and hemodynamic parameters were recorded over time at the following time-points of interest: baseline, bolus 1, hypotension 1, normotension 1, hypertension 1, normotension 2, hypotension 2, bolus 2, hypertension 2 and hypotension 3. The targeted MAP for hypotension ranged from 30 to 50 mmHg. The targeted MAP for normotension ranged from 60 to 80 mmHg. The targeted MAP for hypertension ranged from 90 to 110 mmHg.

2.6. Thermography acquisition and analysis

The left forelimb was held extended with the animal in dorsal recumbency, exposing the elbow and carpus (Fig. 2). These body areas were hairless and not in contact with the heating table. They were also cleaned to remove any residual dirt on the skin before the capture of images.

The thermographic camera (FLIR-E6, FLIR Systems Inc, Wilsonville, Oregon, USA) presented the following characteristics: detector type - uncooled microbolometer, infrared resolution - 160×120 pixels, spectral range - $7.5\text{--}13 \mu\text{m}$, spatial resolution - 5.2 mrad, field of view (FOV) - $45^\circ \times 34^\circ$, object temperature range - -20°C to $+250^\circ\text{C}$, noise equivalent temperature difference (NETD) < 60 mk, thermal Sensitivity < 0.06°C , accuracy $\pm 2\%$ of reading, minimum focus distance - 50 cm. The device was calibrated as recommended by the manufacturer. The camera was positioned and immobilized throughout the procedure 50 cm vertically above the left forelimb. The emissivity of the skin was not measured and was fixed at 0.98, as indicated by the literature in humans [11] and pigs [19]. The reflected apparent temperature was automatically corrected

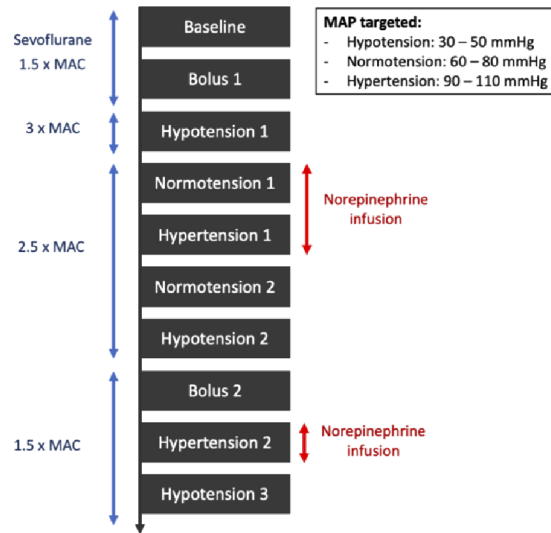


Fig. 1. Study design (MAC: minimum alveolar concentration, MAP: mean arterial pressure).



Fig. 2. Placement of the left foreleg during the study (white arrow: rope placed around the metacarpus to maintain the foreleg).

by the camera. A general description of the working principle of infrared thermography was available elsewhere [20].

Ten snapshots were taken for each pig over time, with one snapshot at each time-point of interest (Fig. 1). The images were taken directly after a fluid bolus or after the target MAP was reached and the hemodynamic parameters were recorded concomitantly.

The images were analyzed *a posteriori* using a dedicated software (Flirtools software). Before every image's analysis, the environmental conditions (humidity, ambient temperature) were recorded beforehand. For carrying out the analysis, a circle of 20 cm² was drawn on the elbow and a circle of 10 cm² was drawn on the carpus. For each zone, the average temperature was calculated by the software (Fig. 3). The core temperature was measured by the PiCCO catheter

and recorded. Gradients between skin temperature of the elbow (T_e) and carpus (T_{ca}) and the central temperature (T_c) were calculated to overcome the changes in skin temperature related to changes in core temperature ($T_c - T_e$) and ($T_c - T_{ca}$). The gradient ($T_e - T_{ca}$) was also calculated, similarly to the gradient $T_{skindiff} = T_{forearm} - T_{fingertip}$ described in human medicine [6]. Conversely to human literature, the peripheral temperature was measured at the carpus and not at the end of the finger to avoid any error due to the rope placed around the metacarpus to maintain the foreleg extended (Fig. 2, Fig. 3). This could have indeed created a tourniquet effect and biased the temperature measurement of the limb's extremity.

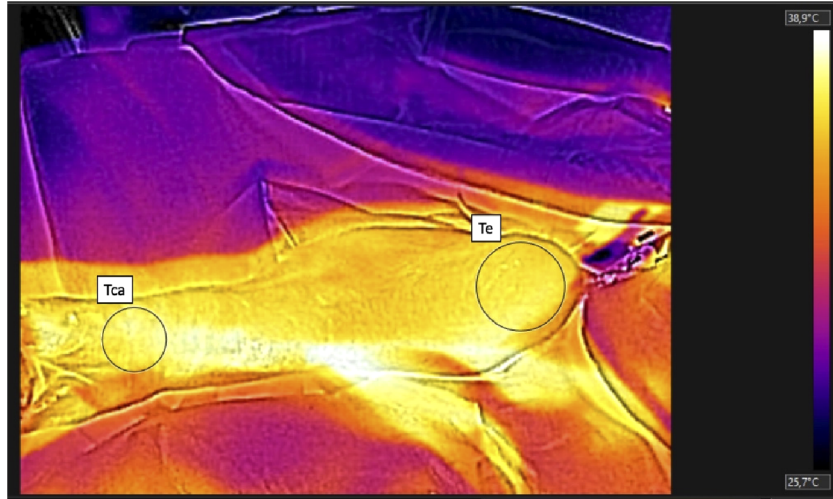


Fig. 3. Analysis of a thermographic image (A circle of 20 cm^2 was drawn on the elbow and a circle of 10 cm^2 was drawn over the *carpus* for the measure of the mean temperature; T_e : elbow mean temperature, T_{ca} : *carpus* mean temperature).

2.7. Statistical analysis

The statistical analysis was performed using R 3.5.2 software (R Foundation for Statistical Computing, Vienna, Austria). The normality of distribution was assessed by using the Shapiro-Wilk normality test. As normal distribution was not corroborated, non-parametric tests were used. Spearman's method was applied to calculate the correlation coefficient between variables. Friedman tests were used for the assessment of intra-group differences. *A posteriori* Dunn's multiple comparisons test was applied to compare the differences between time-points, with a particular focus on "baseline" versus "bolus 1", "bolus 1" versus "hypotension 1", "hypotension 1" versus "hypertension 1", "hypertension 1" versus "hypotension 2", "hypotension 2" versus "bolus 2", and "hypertension 2" versus "hypotension 3". The Bonferroni correction was applied on the p-values generated. Univariate linear mixed models were performed using temperature gradients and T_c as dependent variables, the tested hemodynamic variables as fixed effect and individuals as random effects. Variables with a p-value lower than 0.10 in the univariate analysis were tested in a multivariate linear mixed model. Marginal R squared (R^2), evaluating the proportion of variance explaining by fixed effects, was calculated. To avoid multicollinearity, variables related to each other were not included in the same model. Therefore, hemodynamic variables were chosen over norepinephrine or sevoflurane, stroke volume (SV) and heart rate (HR) over cardiac output and arterial pressure and HR over SI. For every model, homoscedasticity and random distribution of residuals were checked by plotting residuals against fitted value. Random distribution of individual random effect was checked by visualizing the distribution of individual

random intercepts for each model. Data were expressed as median and interquartile range (IQR). A p-value of 0.05 was considered as level of significance.

3. Results

3.1. Descriptive data of hemodynamics and temperature derived parameters

The duration of the experimental procedure for each pig varied between 4 to 5 hours. The mean rate of variation in arterial pressure during the study was estimated at around 1.4 mmHg/min. The median values (IQR) of all variables are presented in Table 1. Due to a rapid change in blood pressure following norepinephrine administration, the measurements for the “normotension 1” period was not performed in two pigs.

3.2. Evolution of temperature gradients and hemodynamic parameters over time

The Friedman test indicated variations over time for (Tc – Te) ($P = 0.0002$), (Tc – Tca) ($P < 0.0001$) and every studied hemodynamics parameters (MAP, SAP, DAP, CI, SI, SVRI, GEDVI, PPV; $P < 0.0001$). No significant difference was found for the evolution of (Te – Tca) ($P = 0.14$).

- *Comparisons between “baseline” and “bolus 1”*

No significant variation was noticed for any parameter

- *Comparisons between “bolus 1” and “hypotension 1”*

A significant decrease of MAP ($P = 0.02$) and a significant increase in PPV ($P = 0.02$) were observed, with non-significant variations of CI, (Tc – Te) and (Tc – Tca) ($P > 0.99$).

- *Comparisons between “hypotension 1” and “hypertension 1”*

A significant increase of MAP ($P = 0.0001$), a significant increase of CI ($P = 0.01$) and a non-significant decrease in PPV ($P = 0.07$), were observed. They were associated with significant decrease of (Tc – Te) and (Tc – Tca) ($P = 0.02$).

- *Comparisons between “hypertension 1” and “hypotension 2”*

A significant decrease of MAP ($P = 0.0001$) was observed, with non-significant variations of CI ($P = 0.13$), PPV ($P > 0.99$), (Tc – Te) ($P = 0.53$) and (Tc – Tca) ($P = 0.22$).

- *Comparisons between “bolus 2” and “hypertension 2”*

A significant increase of MAP ($P = 0.006$), a non-significant increase of CI ($P > 0.99$) and a non-significant decrease in PPV ($P > 0.99$), were observed, associated with non-significant decrease of (Tc – Te) and (Tc – Tca) (respectively $P = 0.67$ and $P = 0.08$).

- *Comparisons between “hypertension 2” and “hypotension 3”*

A significant decrease of MAP ($P = 0.002$) was observed, with no significant variations of CI ($P > 0.99$), PPV ($P > 0.99$), (Tc – Te) ($P = 0.93$) and (Tc – Tca) ($P = 0.47$).

Figure 4 illustrates the evolution of (Tc – Tca), (Tc – Te), MAP, CI and PPV over time.

3.3. Correlations between temperature gradients and hemodynamic parameters

The correlation coefficients and levels of significance are described in Table 2. Among these results, the interesting elements observed are : a fair [21] negative significant correlations were found between MAP and (Tc – Tca) ($r = -0.40$), norepinephrine dose and (Tc – Tca) ($r = -0.42$), norepinephrine dose and (Tc – Te) ($r = -0.40$), CI and (Tc – Te) ($r = -0.32$), CI and (Tc – Tca) ($r = -0.36$), as well as a fair positive significant correlation between VPP and (Tc – Te) ($r = 0.31$).

Table 1. Evolution of the different study parameters over time

	Baseline	Bolus 1	Hypotension 1	Normotension 1	Hypertension 1	Normotension 2
Te-Te °C	2.2 (2.0-2.9)	2.2 (0.6-2.5)	2.5 (1.4-4.1)	2.4 (2.2-3.2)	0.9 (0.2-1.3)^d	1.2 (0.8-2.2)
Te-Tca °C	2.7 (1.9-3.0)	1.7 (0.5-2.7)	2.3 (1.2-3.7)	2.2 (1.4-2.9)	0.5 (0.00-1.2)^d	0.9 (0.4-2.0)
Te-Tca °C	0.2 (-0.4-0.3)	-0.2 (-0.7-0.5)	-0.2 (-0.4-0.1)	-0.6 (-0.9-0.2)	-0.3 (-0.4-0.0)	-0.3 (-0.4-0.1)
MAP mmHg	63 (53-75)	72 (68-78)	42 (39-42)^d	74 (68-78)	103 (96-105)^d	77 (73-78)
CIL-min-m²	1.37 (1.25-1.88)	1.66 (1.31-2.04)	1.34 (1.15-1.51)	1.48 (1.23-5.13)	2.55 (1.75-3.50)^d	2.92 (2.28-3.10)
SI	1.28 (0.87-1.62)	0.97 (0.90-1.25)	1.71 (1.51-2.17)	0.99 (0.91-1.13)	1.03 (0.94-1.24)	1.33 (1.12-1.56)
SVRI dynes-sec-cm⁵-m²	3214 (2700-4289)	3662 (2811-4251)	2554 (2044-2874)	3883 (3083-5480)	3186 (2440-4591)	2137 (1760-2709)
GEDVI mL-m²	189 (186-270)	226 (185-236)	230 (185-259)	248 (205-296)	240 (204-322)	216 (208-271)
PPV %	16 (12-22)	10 (8-12)	20 (19-22)^d	9 (8-10)	10 (8-18)	13 (11-19)
Norépinephrine dose µg.kg.min⁻¹	0 (0-0)	0 (0-0)	0 (0-0)	0.20 (0.15-0.35)	0.50 (0.25-0.80)	0.26 (0.11-0.40)
Sevoflurane dose %	3.5 (3.5-4.6)	3.5 (3.5-4)	8 (8-8)	5.0 (4.6-6.0)	5.0 (5.0-5.0)	5 (3.5-5)
			Hypotension 2	Hypertension 2	Hypotension 3	
Te-Te °C	1.5 (1.2-3.0)	2.1 (1.5-3.3)	2.1 (0.2-1.8)	1.3 (0.2-1.8)	2.1 (1.8-3.5)	
Te-Tca °C	1.4 (0.9-2.6)	2.65 (1.2-3.4)	2.65 (1.2-3.4)	0.9 (0.3-1.5)	2.2 (1.6-2.9)	
Te-Tca °C	-0.2 (-0.4-0.1)	0.1 (-0.5-0.3)	0.1 (-0.5-0.3)	-0.3 (-0.6-0.7)	-0.1 (-0.6-0.1)	
MAP mmHg	43 (30-45)^d	57 (49-60)	57 (49-60)	100 (100-108)^d	48 (46-50)^d	
CIL-min-m²	1.44 (1.29-1.75)	1.54 (1.32-1.76)	1.54 (1.32-1.76)	2.07 (1.50-2.76)	1.69 (1.39-2.22)	
SI	1.85 (1.70-2.34)	1.28 (1.17-1.48)	1.28 (1.17-1.48)	0.91 (0.85-1.00)	1.79 (1.37-2.11)	
SVRI dynes-sec-cm⁵-m²	2459 (2050-2610)	2703 (2446-3542)	2703 (2446-3542)	4065 (3059-5679)	2281 (1898-2756)	
GEDVI mL-m²	178 (172-220)	186 (180-249)	186 (180-249)	207 (182-239)	190 (171-245)	
PPV %	18 (12-23)	7.5 (7-12)	7.5 (7-12)	11 (7-15)	11 (9-16)	
Norépinephrine dose µg.kg.min⁻¹	0 (0-0)	0 (0-0)	0 (0-0)	0.40 (0.20-0.48)	0 (0-0)	
Sevoflurane dose %	5.0 (3.6-5.0)	4.0 (3.5-4.8)	4.0 (3.5-4.8)	3.75 (3.50-5.00)	3.75 (3.50-5.00)	

Tc: Central temperature. Te: elbow temperature. Tca: carpus temperature. MAP: mean arterial pressure. SAP: systolic arterial pressure. DAP: diastolic arterial pressure. CI: cardiac index. SI: shock index. SVRI: systemic vascular resistance index. GEDVI: global end-diastolic volume index. PPV: pulse pressure variation.
^aP < 0.05 for the comparisons of different times: "baseline" versus "bolus 1", "bolus 1" versus "hypotension 1", "hypotension 1" versus "hypertension 1", "hypertension 1" versus "hypotension 2", "hypotension 2" versus "hypertension 2", and "hypertension 2" versus "hypotension 3". Significant results are presented in bold type.

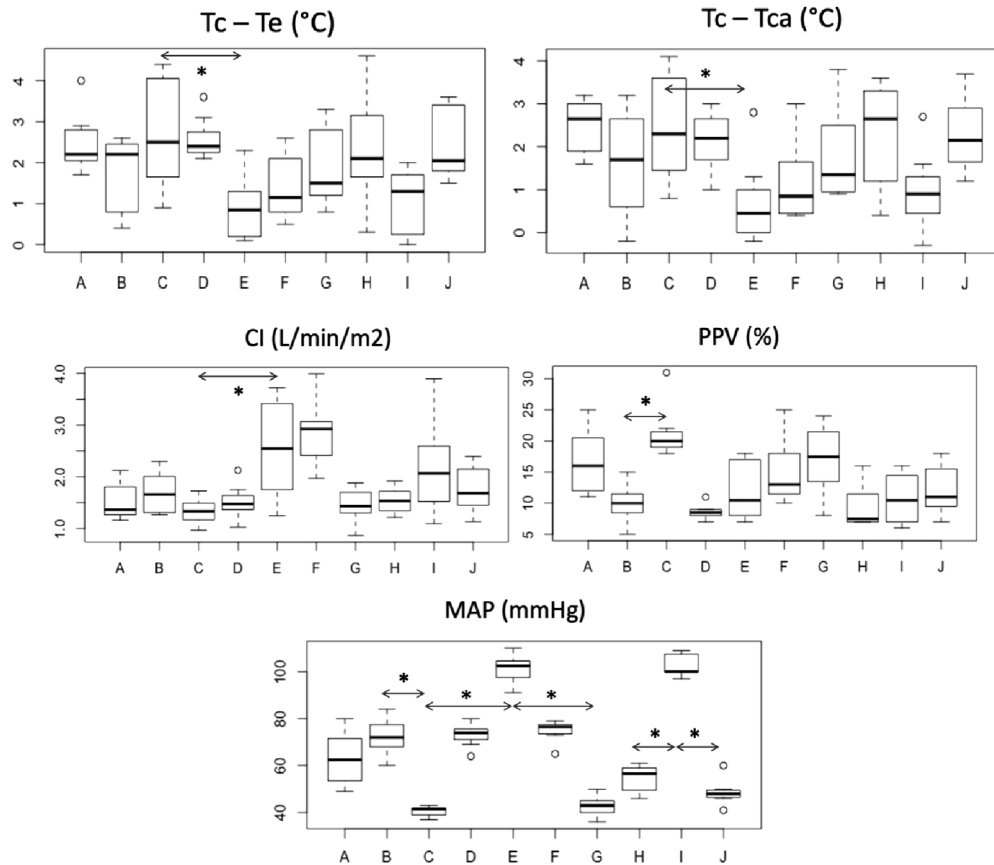


Fig. 4. Boxplots describing the course of $(Tc - Te)$ (a), $(Tc - Tca)$ (b), MAP (c), CI (d) and PPV (e) over time points. On the abscissa: Time points (A: Baseline, B: Bolus 1, C: Hypotension 1, D: Normotension 1, E: Hypertension 1, F: Normotension 2, G: Hypotension 2, H: Bolus 2, I: Hypertension 2, J: Hypotension 3). On ordinate: Tc: central temperature. Te: elbow temperature. Tca: carpus temperature; MAP: mean arterial pressure; CI: cardiac index; PPV: pulse pressure variation, * $P < 0.05$.

Regarding correlations between temperature gradients: there was a very strong positive correlation between $(Tc - Te)$ and $(Tc - Tca)$ and a fair positive correlation between $(Tc - Tca)$ and $(Te - Tca)$.

Figure 5 illustrates $(Tc - Te)$ - $(Tc - Tca)$ as a function of MAP.

3.4. Influence of hemodynamic parameters on temperature gradient

Table 3 summarizes the results of univariate and multivariate linear mixed models. In multivariate analysis, $(Tc - Tca)$ was associated with MAP ($P = 0.004$) and HR ($P = 0.03$), $(Tc - Te)$ was associated with MAP ($P = 0.04$) and HR ($P = 0.01$). No association was demonstrated between hemodynamic parameters and core temperature or $(Te - Tca)$. R^2 for the $(Tc - Tca)$ model was 0.28. Thus, the variation of MAP and HR explain 28% of the variance of $(Tc - Tca)$. R^2 for the $(Tc - Te)$ model was about 0.27. Thus, the variation of SV, MAP and HR explain 27% of the variance of $(Tc - Te)$.

Table 2. Correlations between parameters

		Tc - Te	Tc - Tca	Te - Tca	Tc	Te	Tca
MAP	<i>Spearman correlation</i>	-0.36*	-0.40*	-0.15	0.001	0.27	0.28
	<i>P-value</i>	0.007	0.002	1	1	0.14	0.10
SI	<i>Spearman correlation</i>	0.12	0.19	0.24	0.02	-0.09	-0.15
	<i>P-value</i>	1	0.63	1	1	1	1
CI	<i>Spearman correlation</i>	-0.32*	-0.36*	0.12	-0.007	0.47*	0.47*
	<i>P-value</i>	0.05	0.02	1	1	0.00008	0.00008
SVRI	<i>Spearman correlation</i>	-0.02	-0.05	-0.15	0.001	-0.15	-0.18
	<i>P-value</i>	1	1	1	1	1	1
GEDVI	<i>Spearman correlation</i>	-0.08	-0.001	-0.23	0.20	0.34*	0.40*
	<i>P-value</i>	1	1	0.42	0.78	0.032	0.006
VPP	<i>Spearman correlation</i>	0.31*	0.10	0.19	0.03	-0.28	-0.26
	<i>P-value</i>	0.04	1	0.63	1	0.20	0.30
Norepinephrine dose	<i>Spearman correlation</i>	-0.40*	-0.42*	-0.10	-0.04	0.23	0.25
	<i>P-value</i>	0.002	0.0007	1	1	0.5	0.35
Sevoflurane dose	<i>Spearman correlation</i>	0.07	0.05	-0.04	0.17	0.08	0.07
	<i>P-value</i>	1	1	1	1	1	1
Tc – Te	<i>Spearman correlation</i>	-	0.89*	-0.02	-	-	-
	<i>P-value</i>	-	0.0007	1	-	-	-
Tc – Tca	<i>Spearman correlation</i>	0.89*	-	0.40*	-	-	-
	<i>P-value</i>	0.0007	-	0.002	-	-	-

Tc: central temperature, Te: elbow temperature, Tca: carpus temperature. Correlation coefficient interpretation: fair correlation [$0.30 < |r| < 0.50$], very strong correlation [$0.80 < |r| < 1$] - According to Chan YH. [20]. * $P < 0.05$ (Significant results are presented in bold type)

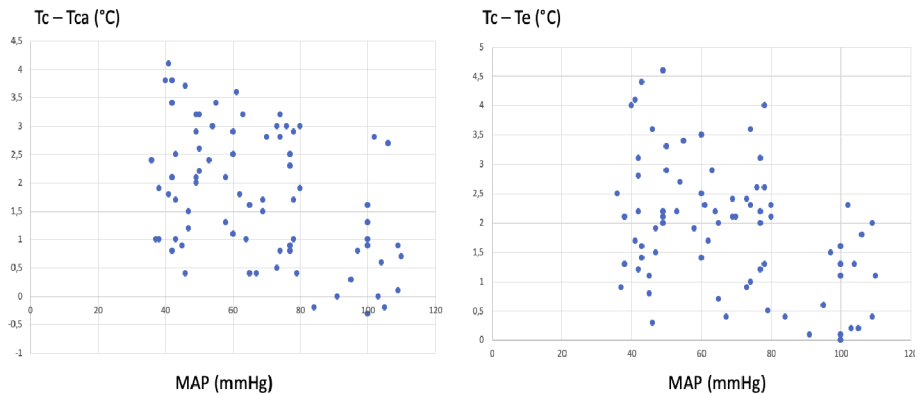


Fig. 5. Representation of (Tc – Tca) and (Tc – Te) as a function of MAP (Tc: central temperature, Te: elbow temperature, Tca: carpus temperature, MAP: mean arterial pressure).

Table 3. Hemodynamic determinants of temperature – Results of univariate and multivariate analysis

Dependent variable	Fixed effect	Univariate analysis		Multivariate analysis	
		Estimate	<i>P</i> -value	Estimate	<i>P</i> -value
Tc - Tca	MAP	-0.024	<0.0001	-0.017	0.004
	GEDVI	-0.005	0.18		
	SV	-0.014	0.12		
	SVRI	-0.0002	0.16		
	HR	-0.021	<0.0001	-0.012	0.03
Tc - Te	PPV	0.033	0.17		
	MAP	-0.024	<0.0001	-0.013	0.04
	GEDVI	-0.004	0.26		
	SV	-0.019	0.06	-0.011	0.19
	SVRI	-0.0001	0.34		
	HR	-0.023	<0.0001	-0.015	0.01
Te - Tca	MAP	-0.0006	0.23		
	GEDVI	-0.0008	0.60		
	SV	0.007	0.06		
	SVRI	<0.0001	0.12		
	HR	0.0008	0.67		
	PPV	0.01	0.27		
Tc	MAP	-0.002	0.58		
	GEDVI	-0.12	0.66		
	SV	-0.006	0.26		
	SVRI	<0.0001	0.46		
	HR	0.004	0.17		
	PPV	-0.0007	0.95		

Tc: Central temperature. Te: elbow temperature. Tca: carpus temperature. HR: heart rate. MAP: mean arterial pressure. SV: stroke volume. SVRI: systemic vascular resistance index. GEDVI: global end-diastolic volume index. PPV: pulse pressure variation. Significant results are presented in bold type.

4. Discussion

The current study aimed to evaluate the variation of IT according to hemodynamic changes in an experimental porcine model. The main results are significant associations between hemodynamic parameters and skin temperature gradients measured with IT. The relationship between IT and hemodynamics parameters were as followed: a fair negative correlation between MAP and $(T_c - T_{ca})$, a fair negative correlation between norepinephrine dose and $(T_c - T_{ca})$ and $(T_c - T_e)$, a fair negative correlation between MAP and $(T_c - T_e)$ and fair negative correlations between these two temperature gradients and CI. Furthermore, MAP and HR significantly influenced $(T_c - T_{ca})$ and $(T_c - T_e)$.

In the current study, a piglet model was chosen as it allows better hemodynamic monitoring and presents physiological similarities with humans, especially regarding cardiovascular physiology [18]. Temperature gradients were chosen, following previous studies that reported the superiority of temperature gradients over single area measurement for the diagnosis of peripheral hypoperfusion in critical patients [6]. The three temperature gradients selected aimed to reproduce the gradients used in human clinical practice. The gradients between the central temperature and the peripheral temperature (elbow or carpus) are very similar to the “central-to-toe” gradient used for human patients. We measured the temperature next to the elbow and the carpus, and not at the end of a finger. As the extremity of the limb was tied to be maintained extended, the perfusion of the fingers and consequently their temperature could have been altered by the rope string acting as a tourniquet. Since a strong correlation between the gradients “ $T_c - T_{ca}$ ” and “ $T_c - T_e$ ” was noticed, it is probable that the measurement of the temperature at the finger level would have given similar results. In addition, former studies have reported the preponderance of heat brought by perfusion over local production [16]. It is now considered that the preponderant role of skin perfusion in the control of temperature is particularly relevant in the acral glabrous areas [10], which justifies the decision to study the cutaneous temperature around the elbow and carpus areas. The calculation of gradients overcomes the influence of central temperature variations that may occur in particular conditions such as anesthesia (excessive heat loss due to anesthetic drugs or heat gain associated with the use of active warming device). Unlike $(T_c - T_{ca})$ and $(T_c - T_e)$, the calculated $(T_e - T_{ca})$ gradient was of little interest: it showed no significant variations over time and no correlation with hemodynamics. This gradient was calculated to reproduce the Tskindiff gradient used in humans as an index of hypoperfusion [6]. This observation confirms hereby previous reports indicating that this gradient lacks reliability to reflect real-time changes in peripheral perfusion [6]. The rapid changes in blood pressure in our experimental setting could explain this absence of significant change over time. Moreover, the $(T_e - T_{ca})$ gradient differed from the one described in human literature, which considers the most peripheral temperature at the end of a finger, whereas in our experimental setting, the carpal temperature was measured for the aforementioned reason.

Regarding hemodynamic variations, the hypotensive phases were performed to mimic the alterations observed during a circulatory shock [2]. The overdose of sevoflurane was chosen as it causes a decrease in systemic vascular resistance and a myocardial depression [22], similarly to the predominant mechanisms of hypotension encountered in septic shock that leads to tissue hypoperfusion [23–25]. To counteract these alterations and promote a progressive increase in blood pressure, norepinephrine was administered because of its predominant agonist effect on α_1 -adreno-receptors and its weak agonist effect on β_1 - β_2 -adreno-receptors (at higher doses), in addition to its short half-life [26]. Fluid challenges were performed to ensure proper blood circulating volume during the pharmacological tests and to limit the dose of vasopressors.

Infrared thermography is easy to perform and does not require an intensive training. The camera used in this study gives instantly the average temperature of an area, allowing a quick calculation of temperature gradients between distinct zones. To date, only a few studies have focused on the use of IT for the diagnosis of peripheral hypoperfusion in critical condition. A

study performed on a porcine model of acute lung injury [27] reported similar results to the present ones. Nevertheless, in this study, the area of interest was different and potentially less appropriate, as it focused on the whole anterior area of the animals and required a complex image processing. Another study aimed to evaluate if IT could help to distinguish survivors and non-survivors during sepsis in human patients. It showed an association between the mottling score and the drop in cutaneous temperature of the knee [5], but thermography was not reported as an independent factor of mortality. In a case series of 8 children, IT was successfully used to distinguish children in shock from healthy children [4]. However, in the study cited previously, no temperature gradient was calculated and the authors did not compare the thermography data with the hemodynamic parameters. Finally, thermography was also studied for the prediction of shock conditions in infants [28]. The objective was to develop an automated system for predicting shock based on a thermal image of a whole infant. A gradient between peripheral to central temperature was calculated using abdominal temperature measured by IT, as a mean to reflect central temperature. Nevertheless, this way of assessing central temperature cannot be considered as a reference technique, contrary to the method used in our study. In this last study, the thermographic data were not compared to hemodynamic parameters and the image analysis procedures were very complex. Thus, our study provides new insights concerning the correlation between hemodynamic parameters and the temperature gradient, which is mostly used in a clinical setting. Furthermore, the technology used in our protocol did not require a complex processing to analyze the images: the results are obtained quickly which may be suitable for a medical practice.

In the current study, there was a significant correlation between the cooling of the extremities and the fall in blood pressure or in cardiac output (Table 2), despite the rapidity of this decline. Furthermore, MAP and HR significantly influence $(T_c - T_{ca})$ and $(T_c - T_e)$. These results confirm the link between blood flow and temperature. The cardiac output equals heart rate time stroke volume. From the results of the multivariate analysis showing the significant association between temperature and heart rate, it seems that the correlation observed with cardiac index is determined more by heart rate than by stroke volume. In addition, the present results suggest that the correlations between MAP, CI and temperature gradients are related to changes in elbow and *carpus* temperature rather than changes in central temperature. Hence, there was no correlation or association between the hemodynamic parameters and the T_c . An increase in MAP and CI may lead ameliorate global tissue perfusion, including skin and other peripheral areas, explaining the observed correlations. Thus, the increase in peripheral perfusion reduce the difference between the central temperature and the peripheral temperature. Furthermore, when blood is flowing from the inner part of the body to the periphery, it mediates a heat transfer. This explains the decrease in calculated temperature gradients reported in our study. In theory, core body heat is produced by basal metabolism and two other main mechanisms (digestion and muscle activity), it is transferred thereafter to the extremities with the bloodstream. The blood therefore gain heat in the core body and then loses thermal energy in peripheral regions, mainly in the skin [17]. In the current study, muscle activity was null and metabolism slowed down. The central temperature was partly maintained artificially by a heating mat placed in the back of the pigs.

Unexpectedly, the marginal R^2 for the models were about 0.28, indicating that only 28% of the cutaneous temperature variance was related to changes in mean arterial pressure, heart rate or stroke volume. This low participation can be explained by the existence of local factors influencing skin temperature, independently from changes in systemic blood pressure [17], but also the peripheral vasodilation caused by sevoflurane [22].

The strong negative correlations between norepinephrine dose and $(T_c - T_e)$ and $(T_c - T_{ca})$ may be explained by the fact that norepinephrine causes an increase in both MAP and CI in our study. A similar finding was observed in pigs undergoing different types of shock (cardiogenic [29], hemorrhagic [30], endotoxic [31]). The mechanisms underlying this raise in MAP are primarily

due to an increase in vascular resistance through α 1-adrenergic receptors stimulation. Regarding the increase in CI, this effect is considered to be mainly related to an increase in venous return and stroke volume following venoconstriction. In addition, β 1-adrenergic stimulation at higher dose may also induce an increase in cardiac contractility [32]. These hemodynamic changes may thus improve peripheral perfusion and explain the correlation observed between the amount of norepinephrine administered and the temperature gradients. The use of norepinephrine could have also caused an increase in peripheral vascular resistances and a potential decrease in the temperature gradient [33], but this was not observed in the present case, probably because of an insufficient dose administered or because of the vasodilation associated with sevoflurane.

Regarding the relationship with other hemodynamic parameters, a moderate positive correlation between PPV and $(T_c - T_e)$ was noticed. Pulse pressure variation results from the difference between the maximum and minimum arterial pressure variations over a single respiratory cycle, it is divided by the mean of the maximum and minimum variations and expressed as a percentage. An increased PPV indicates a relative hypovolemia and predicts fluid responsiveness in humans, but also in pigs [34]. This observation confirms the link between perfusion and temperature. However, despite the potential influence of volemia on the variations of temperature gradients, there was no significant difference between the temperature gradients before and after fluid bolus administration in our study. This counterintuitive result may be explained by the small sample size of our study, the absence of large variations in volemia, or the presence of artefactual increases in PPV related to norepinephrine administration. Indeed, in the pig, PPV has been significantly influenced by norepinephrine infusion [35].

We must acknowledge several limitations for the present study. The small number of animals limited the power of this study and probably explains the absence of significant differences between certain time-points. In particular, failure to observe a significant difference in temperature gradients between “hypertension 1” and “hypotension 2” and between “Hypertension 2” and “Hypotension 3” was an unexpected result. Since the experimental conditions were similar and constant for every animal (the experimental plan, duration of experimentation, environmental conditions and administration of medication), we do not believe that this observation can be explained by modifications of the experimental parameters. It is possible that the rapid successive hemodynamic changes triggered physiological local changes, particularly shear stress and myogenic response [36,37]. So, it is possible that the rapid variations on local vasoreactivity following the administration of sevoflurane and norepinephrine caused some endothelial dysfunction. The results of the linear mixed models were also suggesting the existence local factors influencing skin perfusion.

Another limitation is the absence of method of reference or comparative technique. Despite the fact that IT extremity temperature assessment seems more objective than a manual assessment, we did not compare both methods. Such comparisons were not performed in the afore-mentioned studies. Regarding peripheral perfusion, there is no gold-standard technique [4–6]. Other technologies have been developed, such as NIRS (Near-infrared spectroscopy) and PPI (Peripheral perfusion index) [6,38]. More recently, spectrometry has been used to demonstrate an alteration of peripheral perfusion in a porcine model of hemorrhagic shock [39]. These methods are still under development, but have brought some evidence of impaired peripheral perfusion in critical patients [6]. Unfortunately, we did not have access to these technologies.

The pigs were anesthetized with sevoflurane, an agent that may cause in very rare cases malignant hyperthermia in predisposed pigs [40,41]. An increase in temperature was observed in four piglets, although remaining within normal range, and could have produced a bias. This was limited by the calculation of temperature gradients, that aimed to limit the influence of the variations of central temperature. The occurrence of malignant hyperthermia in the present study is very unlikely, as an increase in EtCO₂ [42], muscle fasciculation and rigidity, which are particular signs of this pathological condition, were not observed in those animals. This

increase in central temperature is probably related to a bad adjustment of the heating mats placed under the pigs. If the use of the heating mats was associated with a risk of influencing the IT measurements, they were used to prevent a decrease of core temperature and were not in direct contact with the forelimb.

Finally, two different temperature measurement techniques were used: thermography for the peripheral temperature and the PiCCO catheter for the core temperature. The accuracy of the thermography camera is about 2% of the measured value (an accuracy of 0.6 to 0.7 °C), while the catheter is more precise (0.15 °C). Thus, in the present study, the accuracy of the calculated temperature gradient was limited by the accuracy of the thermography, that is 0.6 to 0.7 °C. The measurement by the catheter was chosen because of its accuracy and reliability in measuring the core temperature, in addition to its use for hemodynamic monitoring [43].

The impact of time on variations in temperature gradients was not evaluated in our study. There must be a period of time between hemodynamic variations and temperature variations, but this time period could not be evaluated. The experiment consisted in varying the blood pressure over time. The time variable and the pressure variable were likely to be collinear and the inclusion of the two would have reduced the power of the analysis. The average speed of variation of the pressure over time has nevertheless been calculated to illustrate the speed of the variation and provide information concerning the time.

5. Conclusion

The current study provides new insights on the correlation between systemic hemodynamic parameters and the peripheral to central temperature gradients. In the present experimental setting, the peripheral temperature of limb extremities varied according to changes in arterial pressure, heart rate and cardiac index. These temperature changes can be detected by infrared thermography, a non-invasive and easy-to-perform method, and after calculation of a temperature gradient with the central temperature as a reference. These results highlight the possibility of detecting changes of peripheral perfusion by measuring the skin temperature of the extremities by this technology.

Funding

VetAgro Sup.

Disclosures

The authors declare that there are no conflicts of interest related to this article.

References

1. M. Cecconi, D. De Backer, M. Antonelli, R. Beale, J. Bakker, C. Hofer, R. Jaeschke, A. Mebazaa, M. R. Pinsky, J. L. Teboul, J. L. Vincent, and A. Rhodes, "Consensus on circulatory shock and hemodynamic monitoring. Task force of the European Society of Intensive Care Medicine," *Intensive Care Med.* **40**(12), 1795–1815 (2014).
2. J.-L. Vincent and D. De Backer, "Circulatory Shock," *N. Engl. J. Med.* **369**(18), 1726–1734 (2013).
3. Y. Sakr, K. Reinhart, J.-L. Vincent, C. L. Sprung, R. Moreno, V. M. Ranieri, D. De Backer, and D. Payen, "Does dopamine administration in shock influence outcome? Results of the Sepsis Occurrence in Acutely Ill Patients (SOAP) Study," *Crit. Care Med.* **34**(3), 589–597 (2006).
4. A. Ortiz-Dosal, E. S. Kolosovas-Machuca, R. Rivera-Vega, J. Simón, and F. J. González, "Use of infrared thermography in children with shock: A case series," *SAGE Open Med. Case Rep.* **2**, 2050313X1456177 (2014).
5. A. Ferraris, C. Bouisse, N. Mottard, F. Thiollière, S. Anselin, V. Piriou, and B. Allaouchiche, "Mottling score and skin temperature in septic shock: Relation and impact on prognosis in ICU," *PLoS One* **13**(8), e0202329 (2018).
6. M. E. van Genderen, J. van Bommel, and A. Lima, "Monitoring peripheral perfusion in critically ill patients at the bedside," *Curr. Opin. Crit. Care* **18**(3), 273–279 (2012).
7. I. Jawad, I. Lukšić, and S. B. Rafnsson, "Assessing available information on the burden of sepsis: global estimates of incidence, prevalence and mortality," *J. Glob. Health* **2**(1), 010404 (2012).
8. M. Łokaj, N. Czaplá, A. Falkowski, and P. Prowans, "The use of thermography in early detection of tissue perfusion disorders in rats," *Videosurgery Miniinvasive Tech.* **3**(3), 329–336 (2014).

9. A. L. Herrick and A. Murray, "The role of capillaroscopy and thermography in the assessment and management of Raynaud's phenomenon," *Autoimmun. Rev.* **17**(5), 465–472 (2018).
10. J. Allen and K. Howell, "Microvascular imaging: techniques and opportunities for clinical physiological measurements," *Physiol. Meas.* **35**(7), R91–R141 (2014).
11. V. Bernard, E. Staffa, V. Mornstein, and A. Bourek, "Infrared camera assessment of skin surface temperature – Effect of emissivity," *Phys. Med.* **29**(6), 583–591 (2013).
12. H. Motoyama, F. Chen, K. Hijya, T. Kondo, K. Ohata, M. Takahashi, T. Yamada, M. Sato, A. Aoyama, and H. Date, "Novel thermographic detection of regional malperfusion caused by a thrombosis during ex vivo lung perfusion," *Interact. Cardiovasc. Thorac. Surg.* **20**(2), 242–247 (2015).
13. F. Deng, Q. Tang, Y. Zheng, G. Zeng, and N. Zhong, "Infrared thermal imaging as a novel evaluation method for deep vein thrombosis in lower limbs," *Med. Phys.* **39**(12), 7224–7231 (2012).
14. C. Pouzot-Nevolet, A. Barthélemy, I. Goy-Thollot, E. Boselli, M. Cambournac, J. Guillaumin, J.-M. Bonnet-Garin, and B. Allaouchiche, "Infrared thermography: a rapid and accurate technique to detect feline aortic thromboembolism," *J. Feline Med. Surg.* **20**(8), 780–785 (2018).
15. M. Adam, E. Y. K. Ng, J. H. Tan, M. L. Heng, J. W. K. Tong, and U. R. Acharya, "Computer aided diagnosis of diabetic foot using infrared thermography: A review," *Comput. Biol. Med.* **91**, 326–336 (2017).
16. T. J. Love, "Thermography as an Indicator of Blood Perfusion," *Ann. N. Y. Acad. Sci.* **335**(1 Thermal Chara), 429–437 (1980).
17. B. F. Jones, "A reappraisal of the use of infrared thermal image analysis in medicine," *IEEE Trans. Med. Imaging* **17**(6), 1019–1027 (1998).
18. M. M. Swindle, A. Makin, A. J. Herron, F. J. Clubb, and K. S. Frazier, "Swine as Models in Biomedical Research and Toxicology Testing," *Vet. Pathol.* **49**(2), 344–356 (2012).
19. D. D. Soerensen, S. Clausen, J. B. Mercer, and L. J. Pedersen, "Determining the emissivity of pig skin for accurate infrared thermography," *Comput. Electron. Agric.* **109**, 52–58 (2014).
20. G. J. Tattersall, "Infrared thermography: A non-invasive window into thermal physiology," *Comp. Biochem. Physiol., Part A: Mol. Integr. Physiol.* **202**, 78–98 (2016).
21. Y. H. Chan, "Biostatistics104: Correlational Analysis," *Singapore Med. J.* **44**(12), 614–619 (2003).
22. S. De Hert and A. Moerman, "Sevoflurane," *F1000Research* **4**, 626 (2015).
23. J. A. Russell, B. Rush, and J. Boyd, "Pathophysiology of Septic Shock," *Crit. Care Clin.* **34**(1), 43–61 (2018).
24. R. Sato and M. Nasu, "A review of sepsis-induced cardiomyopathy," *J. Intensive Care* **3**(1), 48 (2015).
25. M. M. Gamkrelidze, N. A. Intskirveli, K. D. Vardosanidze, K. E. Chikhladze, L. S. Goliadze, and L. R. Ratiani, "Vasoplegia in septic shock (review)," *Georgian Med. News* **239**, 56–62 (2015).
26. S. P. H. Alexander, A. Mathie, and J. A. Peters, "Guide to Receptors and Channels (GRAC), 5th edition," *Br. J. Pharmacol.* **164**(Suppl 1), S1–S2 (2011).
27. C. B. Pereira, M. Czaplak, N. Blantik, R. Rossaint, V. Blazek, and S. Leonhardt, "Contact-free monitoring of circulation and perfusion dynamics based on the analysis of thermal imagery," *Biomed. Opt. Express* **5**(4), 1075–1089 (2014).
28. A. Nagori, L. S. Dhingra, A. Bhatnagar, R. Lodha, and T. Sethi, "Predicting Hemodynamic Shock from Thermal Images using Machine Learning," *Sci. Rep.* **9**(1), 91 (2019).
29. A. Beurton, N. Ducrocq, T. Auchet, F. Joineau-Groubatch, A. Falanga, A. Kimmoun, N. Girerd, R. Fay, F. Vanhuysse, N. Tran, and B. Levy, "Beneficial Effects of Norepinephrine Alone on Cardiovascular Function and Tissue Oxygenation in a Pig Model of Cardiogenic Shock," *Shock* **46**(2), 214–218 (2016).
30. R. Giraud, N. Siegenthaler, D. Arroyo, and K. Bendjelid, "Impact of epinephrine and norepinephrine on two dynamic indices in a porcine hemorrhagic shock model," *J. Trauma Acute Care Surg.* **77**(4), 564–569 (2014).
31. M. M. Treggiari, J.-A. Romand, D. Burgener, P. M. Suter, and A. Aneman, "Effect of increasing norepinephrine dosage on regional blood flow in a porcine model of endotoxin shock," *Crit. Care Med.* **30**(6), 1334–1339 (2002).
32. R. Persichini, S. Silva, J.-L. Teboul, M. Jozwiak, D. Chemla, C. Richard, and X. Monnet, "Effects of norepinephrine on mean systemic pressure and venous return in human septic shock," *Crit. Care Med.* **40**(12), 3146–3153 (2012).
33. P. Foulon and D. De Backer, "The hemodynamic effects of norepinephrine: far more than an increase in blood pressure!" *Ann. Transl. Med.* **6**(S1), S25 (2018).
34. J. Noel-Morgan, D. Otsuki, J. O. Auler, J. Fukushima, and D. Fantoni, "Pulse Pressure Variation Is Comparable With Central Venous Pressure to Guide Fluid Resuscitation in Experimental Hemorrhagic Shock With Endotoxemia," *Shock* **40**(4), 303–311 (2013).
35. J. Renner, P. Meybohm, R. Hanss, M. Gruenewald, J. Scholz, and B. Bein, "Effects of norepinephrine on dynamic variables of fluid responsiveness during hemorrhage and after resuscitation in a pediatric porcine model," *Paediatr. Anaesth.* **19**(7), 688–694 (2009).
36. K. S. Cunningham and A. I. Gotlieb, "The role of shear stress in the pathogenesis of atherosclerosis," *Lab. Invest.* **85**(1), 9–23 (2005).
37. P. F. Davies, "Hemodynamic shear stress and the endothelium in cardiovascular pathophysiology," *Nat. Clin. Pract. Cardiovasc. Med.* **6**(1), 16–26 (2009).
38. T. Li, M. Duan, K. Li, G. Yu, and Z. Ruan, "Bedside monitoring of patients with shock using a portable spatially-resolved near-infrared spectroscopy," *Biomed. Opt. Express* **6**(9), 3431 (2015).
39. K. Vishwanath, R. Gurjar, D. Wolf, S. Riccardi, M. Duggan, and D. King, "Diffuse optical monitoring of peripheral tissues during uncontrolled internal hemorrhage in a porcine model," *Biomed. Opt. Express* **9**(2), 569–580 (2018).

40. G. A. Gronert and J. H. Milde, "Variations in onset of porcine malignant hyperthermia," *Anesth. Analg.* **60**(7), 499–503 (1981).
41. M. Shulman, B. Braverman, A. D. Ivankovich, and G. Gronert, "Sevoflurane triggers malignant hyperthermia in swine," *Anesthesiology* **54**(3), 259–260 (1981).
42. H. Rosenberg, N. Pollock, A. Schiemann, T. Bulger, and K. Stowell, "Malignant hyperthermia: a review," *Orphanet J. Rare Dis.* **10**(1), 93 (2015).
43. D. Krizanac, P. Stratil, D. Hoerburger, C. Testori, C. Wallmueller, A. Schober, M. Haugk, M. Haller, W. Behringer, H. Herkner, F. Sterz, and M. Holzer, "Femoro-iliacal artery versus pulmonary artery core temperature measurement during therapeutic hypothermia: an observational study," *Resuscitation* **84**(6), 805–809 (2013).